J Mater Sci (2021) 56:513–527

Computation & theory

Artificial neural networks test for the prediction of chemical stability of pyroclastic deposits-based AAMs and comparison with conventional mathematical approach (MLR)

Claudio Finocchiaro[1], Germana Barone[1,*], Paolo Mazzoleni[1], Caterina Sgarlata[2], Isabella Lancellotti[2], Cristina Leonelli[2], and Marcello Romagnoli[2]

[1] Department of Biological, Geological and Environmental Sciences, University of Catania, Corso Italia, 57, 95127 Catania, Italy
[2] Department of Engineering "Enzo Ferrari", University of Modena and Reggio Emilia, Via Pietro Vivarelli 10, 41125 Modena, Italy

Received: 28 May 2020
Accepted: 10 August 2020
Published online: 16 September 2020

ABSTRACT

The investigation on the reticulation degree of volcanic alkali-activated materials, AAMs, were experimentally determined in terms of chemico-physical properties: weight loss after leaching test in water, ionic conductivity and pH of the leachate and compressive strength. Artificial neural network (ANN) was successfully applied to predict the chemical stability of volcanic alkali-activated materials. Nine input data per each chemico-physical parameter were used to train each ANN. The training series of specific volcanic precursors were tested also for the other one. Excellent correlations between experimental and calculated data of the same precursor type were found reaching values around one. The evidence of strong effect on chemical stability of the alkaline activator SiO_2/Na_2O molar ratio as well as the Si/Al ratio of precursor mixtures on the reticulation degree of ghiara-based formulation with respect to volcanic ash-based materials is presented. It must be noted that such effect was much less pronounced on the compressive strength values, appearing more insensitive the molar ratio of the alkaline activator. The comparison of the ANN results with more conventional multiple linear regression (MLR) testifies the higher prediction performance of the first method. MLRs results, less significant, are useful to confirm the powerful capacity of ANNs to identify the more suitable formulation using a set of experimental AAMs. This study, as few others, on the correlation between chemical stability and compressive strength of AAMs provide a great contribution in the direction of durability and in-life mechanical performance of these class of materials.

Handling Editor: Yaroslava Yingling.

Address correspondence to E-mail: gbarone@unict.it

https://doi.org/10.1007/s10853-020-05250-w

GRAPHIC ABSTRACT

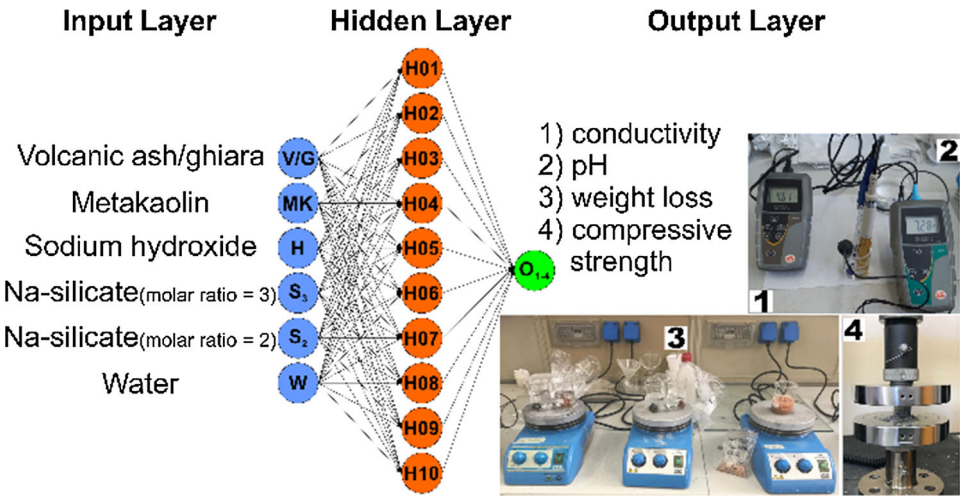

Introduction

Alkali-activated aluminosilicate polymers, otherwise known as geopolymers and proposed for the first time by Davidovits [1], represent a valid alternative to the common construction materials thanks to low-energy-consuming and cost-efficient process, making them strongly versatile [2–5]. Moreover, their production process became of high interest for sustainable management of waste materials, which are used as precursors or waste to be encapsulated in addition to an alkaline solution [6–8]. Until now, according to Italian National legislation, a volcanic deposit caused by explosive eruptions represents a natural waste material which requires specific managing protocol and consequently high cost of management [9]. Indeed, the fresh particles, once erupted, require treatments to remove chlorides and sulphates deposited on their surfaces [10] before to be used in small amount as aggregates to produce traditional mortars [9]. However, volcanic particles thanks to their high amorphous and aluminosilicate contents are known as suitable precursors for alkali-activated binder production [11–13], regardless they require thermal treatments or metakaolin addition as additive component to reduce the setting time caused by the high volcanic glass stability in alkaline environment [14]. In this scenario, volcanic ash and volcanic paleo-soils, the latter locally known with *ghiara* term [15–20] and coming from Mt. Etna volcano (Sicily, Italy), were used in binary mixture with small metakaolin amount additions, allowing an alkaline activation at room temperature with the aim to produce geopolymeric binders to apply in situ cultural heritage interventions [21]. In general, the final physical properties of alkali-activated materials (AAMs) are strongly influenced by different variables, such as SiO_2/Al_2O_3, Na/Al and solid/liquid ratios [22, 23], especially when aluminosilicate sources, as in this work, are natural waste materials, characterized by an intrinsic heterogeneity.

Among all methods, artificial neural networks (ANNs) are used and appreciated for materials science [24–28], although geopolymer field is still few explored despite a high request of a mix design tool able to predict formulations with excellent chemical stability features. Generally, ANNs have been focused on predict mechanical behaviour [29–33] and abrasion resistance [34] of geopolymer materials. However, none of the ANNs have been applied to AAMs based on volcanic residues until now.

Therefore, in this work, ANNs were test for the first time to AAMs based on pyroclastic deposits from Mt. Etna volcano, Italy, evaluating physical properties, such as weight loss during leaching

treatments in water, ionic conductivity and pH of the leachate solution, and compressive strengths, which are all strongly influenced by the chemical stability of final product. Traditional multiple linear regressions (MLR) were also implemented to compare the correlation found with ANNs, aiming to highlight the strength points of predictive approaches used. Our ANN predictive approach can be defined useful to provide an optimization of mix design for AAMs based on volcanic particles with great durability features and to promote the potentiality of this kind of building materials still without market rules, but very appreciate by scientific community.

Materials and methods

Materials and sample preparation

Eighteen binary mixtures made of volcanic ash (indicated with "V") or ghiara paleo-soil ("G"), whose sampling details and characterization results are reported in [21], with small and progressive increases (10–25 wt% on the solid total weight) of metakaolin (MK), commercialized as ARGICAL^{TM} M1000 (provided by IMERYS, France) [35] and two different sodium-activating solutions were considered. These latter are differentiated by the type and the quantity of sodium silicate used: (1) a combination of sodium hydroxide (8 M) and sodium silicate, provided by Ingessil s.r.l., Italy, with a molar ratio $SiO_2/Na_2O = 3$; (2) a different sodium silicate (code: 373908), provided by Carlo Erba, Italy, with a molar ratio $SiO_2/Na_2O = 2$, maintaining constant the quantity of sodium hydroxide (8 M). Therefore, the samples considered for the ANNs and MLR implementations are labelled as following: VM/GM_3-10/25 and VM/GM_2-10/25, indicating with the subscript the type of silicate according to the SiO_2/Na_2O molar ratio. Moreover, for VM/GM_2 series, a formulation with lower silicate amount, labelled VM/GM_2-20LS, was considered. All the formulations with corresponding labels are reported in Table 1. The same preparation steps were adopted for all series to make them comparable. It was deeply explained in the previous work [21], as well as the characterization results of the samples belonging to VM/GM_2 series, differently for the results of VM/GM_3 series which are reported for the first time in this work.

Experimental methods

The eighteen samples of both series were characterized with the aim to assess the chemical stability in aqueous environment evaluating the consolidation performance after alkaline activation. Therefore, the pH and the ionic conductivity test were performed on the solutions following the immersion of samples, after 28 room temperature curing days, at 25 °C in de-ionized water. The ionic conductivity measures the solution's electrical conductivity which is influenced by the motion of all the free ionic charges released in the solutions and thus strongly depending on the total dissolved solid.

Therefore, solid shreds of samples were immersed in distilled water with a solid/liquid ratio of 1/10 in stirring conditions for 24 h in a beaker. Measurements were determined for different times 0, 5, 15, 30, 60, 120, 720 and 1440 min, evaluating the values changes over the 24 h as results of amount of dissolved solid [21]. At the same time, the weight loss after water treatments in stirring condition were evaluated, comparing the initial (w_i) and the final (w_f) weights, whose values are expressed in percentage according to the following equation:

$$\text{weight loss}(\%) = \frac{w_i - w_f}{w_i} \times 100$$

Compressive strength was determined using an Instron 5567 Universal Testing Machine with 30 kN load limit and displacement of 3 mm/min according to the standard UNI EN 826 on four cubic samples (2 × 2x2 cm^3) of each formulation cured at 28 days.

Analysis approaches: ANN and MLR

ANN principles

ANNs are computational modelling tools used in complex problem solving tasks organized with dense architectures, highly interconnected by simple computing elements (called artificial neurons or nodes) capable to perform parallel computations for data processing [36, 37]. ANNs find analogies with those of human brain network. In detail, they are arranged based on a hierarchical structure with three main layers: input layer, hidden layer (one or more) and output layer, linked through weighted connections (i.e. values) [38–40]. Each node calculates the effect of

Table 1 Labels and formulation details (in wt%) of the experimentally prepared AAMs

Sample	V or G (%)	MK (%)	NaOH (8 M) (%)	Na_2SiO_3 (SiO_2/Na_2O = 3) (%)	Na_2SiO_3 (SiO_2/Na_2O = 2) (%)	H_2O (%)
VM_3-10	68.18	7.58	2.24	5.45	0.00	16.56
VM_3-15	64.39	11.36	2.24	5.45	0.00	16.56
VM_3-20	60.61	15.15	2.24	5.45	0.00	16.56
VM_3-25	56.82	18.94	2.24	5.45	0.00	16.56
VM_2-10	59.21	6.58	1.94	0.00	12.89	19.37
VM_2-15	55.92	9.87	1.94	0.00	12.89	19.37
VM_2-20	52.63	13.16	1.94	0.00	12.89	19.37
VM_2-25	49.34	16.45	1.94	0.00	12.89	19.37
VM_2-20LS	57.14	14.29	2.11	0.00	9.80	16.66
GM_2-10	62.50	6.94	2.05	0.00	10.89	17.62
GM_2-15	59.03	10.42	2.05	0.00	10.89	17.62
GM_2-20	55.56	13.89	2.05	0.00	10.89	17.62
GM_2-25	52.08	17.36	2.05	0.00	10.89	17.62
GM_2-20LS	57.14	14.29	2.11	0.00	9.80	16.66
GM_3-10	68.18	7.58	2.24	5.45	0.00	16.56
GM_3-15	64.39	11.36	2.24	5.45	0.00	16.56
GM_3-20	60.61	15.15	2.24	5.45	0.00	16.56
GM_3-25	56.82	18.94	2.24	5.45	0.00	16.56

inputs and weights through the sum function, which calculates the net input linked to a neuron [31]. The weighted sums of the input components $(net)_j$ are calculated using the following equation:

$$(\text{net})_j = \sum_{i=1}^{n} W_{ij} x_i + b \quad (1)$$

where $(net)_j$ is the weighted sum of the jth neuron for the input received from the preceding layer with n neurons, W_{ij} is the weight between the jth neuron in the previous layer, x_i is the output of the ith neuron in the previous layer [41], b is a fix value, and $\sum$ represents sum function.

Activation function is a function that processes the net input obtained from sum function and determines the neuron output. In general, for multilayer feedforward models as the activation function, sigmoid activation function is used. The output of the jth neuron $(out)_j$ is computed with a sigmoid activation function using the following equation [42]:

$$O_j = f(\text{net})_j = \frac{1}{1 + e^{-\alpha(\text{net})_j}} \quad (2)$$

where α is constant used to control the slope of the semi-linear region. The sigmoid nonlinearity activates in every layer except in the input layer [42]. The sigmoid activation function represented by Eq. (2) gives outputs in (0, 1). If it desired, the outputs of this function can be adjusted to (−1, 1) interval. As the sigmoid processor represents a continuous function, it is particularly used in nonlinear descriptions. Because its derivatives can be determined easily with regard to the parameters within $(net)_j$ variable [41]. However, these connections need to be trained to induce the input variables to the expected results in agreement with the experimental ones through continuous iterations [43, 44], computed for example using a feedforward-backpropagation neural network aimed to minimize the total error or mean error of target computed by the neural network [45].

ANN design

Four ANNs for each physical parameter (weight loss, conductivity, pH and compressive strengths), measured during the laboratory experiments with the same measuring setting, were implemented using the design reported in Table 2. ANN model has 6 neurons in the input layer, ten neurons in one hidden layer and one neuron as output layer as schematically plotted in Fig. 1. The mix design of each formulation was used as input data, considering the volcanic precursor, metakaolin, sodium hydroxide, water, sodium silicate type and amounts (Table 3). In detail, the ANNs were created according to the type of volcanic precursor (i.e. V-ANNs and G-ANNs). Moreover, these latter were used as training series for

the opposite one with the aim to observe affinities among these pyroclastic materials (i.e. V-ANNs were used to predict GM samples and vice versa). The neurons of neighbouring layers are completely interconnected by weights. The software used was NNpred, a freeware MS-Excel implementation developed by Angshuman Saha [46] and extensively used across many field and academia. A feedforward-backpropagation neural network with a sigmoid activation function was used. Momentum rate and learning rate values did not optimise, but the default values were used for model training. NNpred is set by the developer to perform only 500 training cycles, but it was forced to carry out 5000 epochs with the aim to obtain a better fitting, thus, to reach the least training error. This latter can be reached after epoch nr. 5000 or lower depend on the setting and/or dataset and, generally, already after few tens of epochs, the training error decreases of much.

MLR principles

Through the regression analysis, the dependent variables (Y) are evaluated considering the variations of independent variables (X_m), with the aim to determine which one has a significant impact. According to the relationship between the dataset, a straight-line regression is the commonly used. In statistics, a linear regression is defined by the following mathematical equation:

$$Y_i = \beta_0 + \beta_1 X_1 + \ldots + \beta_n X_n + \varepsilon$$

where Y_i = dependent variable, X_m = explanatory variables, β_0 = y-intercept (constant term), β_{m-} = slope coefficient of m-th explanatory variable, ε = the model's error term (also known as the residuals) which is the difference between the value of dependent value and the expected one [47].

Table 2 Parameters used in ANNs

Network architecture	
Number of inputs	6
Number of hidden layers	1
Hidden layer size	10
Number of outputs	1
Learning parameter (range 0–1)	0.4
Momentum (range 0–1)	0
Number of training cycles	5000
Training Mode	Sequential

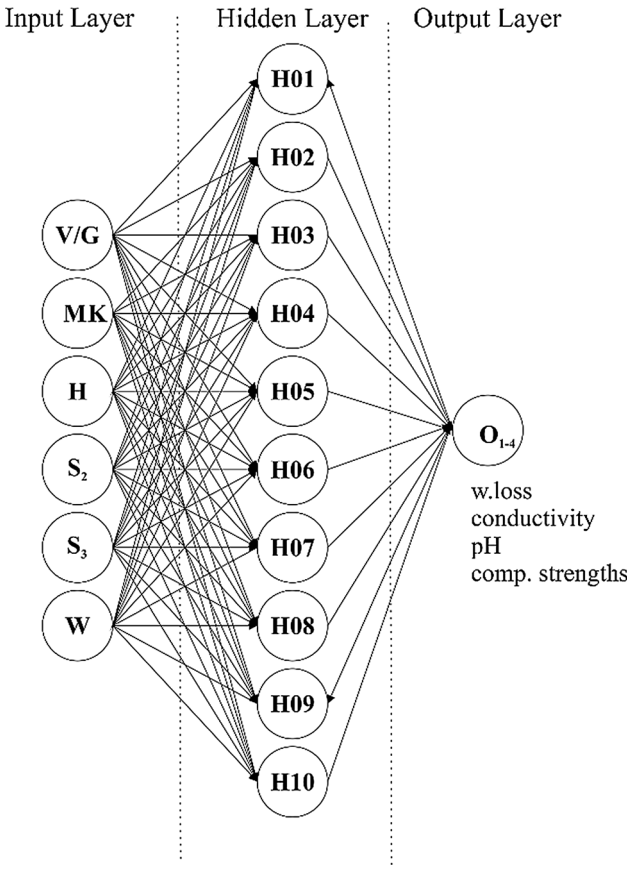

Figure 1 ANN model used: neuron (circle) and weight (arrow). Input layer: volcanic ash/ghiara (V/G); metakaolin (MK); sodium hydroxide (H); sodium silicate with SiO_2/Na_2O = 2 (S_2); sodium silicate with SiO_2/Na_2O = 3 (S_3); water (W). Hidden layer (H01-10); Output layer (O_{1-4}): weight loss, conductivity, pH and compressive strengths.

MLR design

Two set of multiple linear regressions (MLR) were implemented, labelled V-MLR and G-MLR, respectively, for volcanic ash and ghiara precursors. The independent variables were chosen among the type of reactants involved in each formulation considering significant influences on dependent ones (i.e. weight loss, conductivity, pH and compressive strengths). In this scenario, all reactants used for alkaline activation were considered except the sodium hydroxide and the sodium silicate with molar ratio equal to three (S_3) which resulted statistically insignificant on dependent variables due to: (1) the constant amount of NaOH used in all formulations; (2) the constant amount of S_3 in VM_3 and GM_3 series contrary to the other series (Table 3).

Table 3 Summary with input data (wt% reactants) and output data (experimental results)

Sample	Input data						Output data (experimental)			
	V or G (%)	MK (%)	NaOH (8 M) (%)	$Na_2SiO_3(SiO_2/Na_2O = 3)$ (%)	$Na_2SiO_3(SiO_2/Na_2O = 2)$ (%)	Tot. H_2O (%)	O_1 weight loss (%)	O_2 Conductivity (mS/m)	O_3 pH	O_4 Comp. Strength (MPa)
VM_3-10	68.18	7.58	2.24	5.45	0.00	16.56	1.76	312	9.3	24.77
VM_3-15	64.39	11.36	2.24	5.45	0.00	16.56	5.18	372	9.5	37.79
VM_3-20	60.61	15.15	2.24	5.45	0.00	16.56	0.87	245	8.6	32.58
VM_3-25	56.82	18.94	2.24	5.45	0.00	16.56	0.91	261	8.5	39.59
VM_2-10	59.21	6.58	1.94	0.00	12.89	19.37	5.95	574.1	12.2	14.27
VM_2-15	55.92	9.87	1.94	0.00	12.89	19.37	4.68	574	12.2	15.32
VM_2-20	52.63	13.16	1.94	0.00	12.89	19.37	4.15	504	12.0	23.3
VM_2-25	49.34	16.45	1.94	0.00	12.89	19.37	3.23	261.1	12.0	38.03
VM_2-20LS	57.14	14.29	2.11	0.00	9.80	16.66	3.94	261.2	11.8	34.21
GM_2-10	62.50	6.94	2.05	0.00	10.89	17.62	5.56	598	12.0	10.84
GM_2-15	59.03	10.42	2.05	0.00	10.89	17.62	4.38	648	12.2	15.09
GM_2-20	55.56	13.89	2.05	0.00	10.89	17.62	2.92	569	12.1	25.27
GM_2-25	52.08	17.36	2.05	0.00	10.89	17.62	1.76	454	12.1	37.9
GM_2-20LS	57.14	14.29	2.11	0.00	9.80	16.66	2.33	536	12.1	32.21
GM_3-10	68.18	7.58	2.24	5.45	0.00	16.56	1.84	331	9.0	16.87
GM_3-15	64.39	11.36	2.24	5.45	0.00	16.56	0.93	337	9.1	21.93
GM_3-20	60.61	15.15	2.24	5.45	0.00	16.56	0.87	265	9.2	27.65
GM_3-25	56.82	18.94	2.24	5.45	0.00	16.56	0.58	173	8.8	40.54

These latter include the results of chemical stability test (weight loss, ionic conductivity and pH) and compressive strengths after 28 curing days. The errors of each equipment are: 0.01 g referred to balance sensitivity for weight loss; ± 1% full scale accuracy for ionic conductivity; ± 0.1 pH; standard deviation was calculated for compressive strength. The double line divides the samples according to V/G-ANNs. The results of VM/GM_2 are reported from [21]

MLRs were performed using Excel tool "Data Analysis → regression" based on the *least square method*, with the goal to obtain the smallest possible squares sum and draw a line closest to the data. The interpretation of MLR was carried out considering the determination coefficient R squared (range value

0–1), indicator of the goodness of the adaptation, the R-squared adjusted coefficient takes into account the independent variables number in the model with the aim to obtain both values much close each other and finally, the significance (F) of variance analysis to statistically quantify the reliability of the obtained results. Generally, this latter should be less than 0.05 (5%) to demonstrate the goodness of the model used.

Results and discussion

Experimental results

The obtained results of all the series were reported in Table 3. Briefly, the results showed a general progressive decreasing of weight loss, conductivity and pH values at increasing metakaolin content in the mixture, contrary to the compressive strengths which increases increasing MK content. VM_3-15 sample highlighted contrasting values in comparison with the entire trend, maybe due to instrumental error or preparation one. In this scenario, we consider it marginally. Therefore, according to these results, a better reticulation was reached in the samples with higher metakaolin amount, demonstrating the positive influence as additive component due to the optimization of Si/Al ratio with the aim to obtain binders at room temperature as in situ interventions. By comparing the series activated with alkaline solution with $SiO_2/Na_2O = 3$ and with $SiO_2/Na_2O = 2$, it appears evident the improvement of all the properties for ratio = 3. This is an important finding because it means such ratio strongly influences the reticulation as well as the leaching of ionic species in water, while the effect on compressive strength is not so evident. In particular, all the chemical properties such as weight loss, pH and conductivity decrease for ratio 3, indicating the formation of a more stable matrix, with a correlated increase in mechanical properties.

A study of such trend with statistical model will allow a deeper understanding and quantification of the role of the alkaline solution and the aluminosilicate precursor (see next paragraph).

ANNs results

V-ANNs

The V-ANNs trained with the input data of VM samples show an excellent capacity to predict the experimental data. Figure 2 plots the correlations between the experimental (x axis) and calculated (y axis) data for each physical property by VM input data. Indeed, the high determination coefficients (R^2) of each trendline confirm the good fitting. Moreover, the correlation coefficients of each physical property are almost equal to one (Table 4). Differently, the previsions on calculated data of GM samples driven by VM training data show, in general, a discrete predicting capacity (Fig. 3) with a correlation coefficient ranging around 0.53–0.98. In particular, the pH is the best predicted variable (Fig. 3c), while the conductivity the worst among all the material properties considered (Fig. 3b).

Concerning the chemical stability results, in the prediction of ionic conductivity (Fig. 2b) and pH (Fig. 2c), the V-ANNs tends to linearize the results for the V-AAMs series, leaving the VM_3-15 values out of trendline as expected. The G-ANNs plots using VM-training overestimate the ionic conductivity for the GM_3 series while underestimate the GM_2 series (Fig. 3b). This means that the alkaline solution with SiO_2/Na_2O molar ratio of 3 had a much stronger reticulation effect, i.e. lower conductivity values, on ghiara-based AAMs with respect to volcanic ash, that appeared almost insensitive to such molar ratio. Similar considerations can be deduced for the weight loss plot (Fig. 3a), where GM_3 series have values overestimated. Also, in this case, the alkali activator had a more efficient role of consolidating the geopolymeric matrix in the ghiara-based materials with respect to the volcanic ash. The comparison of such ANNs results provide an interesting support to the interpretation of the role of the two different alkaline solutions used as activators for the production of alkali-activated materials. In particular, the ghiara-based formulation reacted much better in the SiO_2/Na_2O molar ratio = 3 conditions, while in the volcanic ash-base materials, the reactivity is mainly due to the metakaolin fraction and proceed with the linearity expected from the % amount of MK in the mixture whatever the alkaline solution is used.

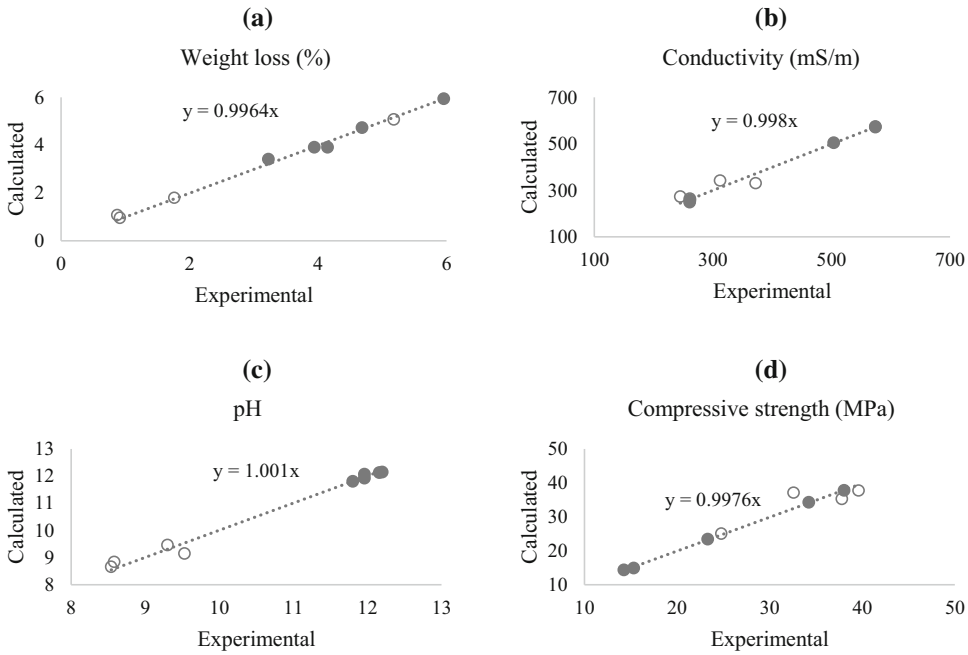

Figure 2 V-ANNs plots for each ANN created: **a** weight loss; **b** conductivity; **c** pH; **d** average compressive strengths. The dashed line indicates the trendline passing for the origin. Legends: filled circle VM_2 series open circle VM_3 series.

Table 4 Correlation between experimental and calculated data using V-training

Sample	Experimental data				Calculated data			
	weight loss (%)	Conductivity (mS/m)	pH	Comp. Strength (MPa)	weight loss (%)	Conductivity (mS/m)	pH	Comp. Strength (MPa)
VM_3-10	1.76	312	9.3	24.77	1.80	342.3	9.5	25.09
VM_3-15	5.18	372	9.5	37.79	5.08	330.8	9.1	35.31
VM_3-20	0.87	245	8.6	32.58	1.09	273.6	8.8	37.15
VM_3-25	0.91	261	8.5	39.59	0.97	249.1	8.7	37.79
VM_2-10	5.95	574.1	12.2	14.27	5.95	573.9	12.1	14.34
VM_2-15	4.68	574	12.2	15.32	4.73	572.3	12.1	14.86
VM_2-20	4.15	504	12.0	23.3	3.91	504.3	12.1	23.38
VM_2-25	3.23	261.1	12.0	38.03	3.41	264.6	11.9	37.80
VM_2-20LS	3.94	261.2	11.8	34.21	3.92	258.1	11.8	34.25
				Corr. Coef	0.998	0.988	0.994	0.980
GM_3-10	1.84	331	9.0	16.87	1.85	342.3	9.5	25.09
GM_3-15	0.93	337	9.1	21.93	5.03	330.8	9.1	35.31
GM_3-20	0.87	265	9.2	27.65	1.10	273.6	8.8	37.15
GM_3-25	0.58	173	8.8	40.54	1.00	249.1	8.7	37.79
GM_2-10	5.56	598	12.0	10.84	5.95	562.4	12.1	14.39
GM_2-15	4.38	648	12.2	15.09	5.89	457.7	12.1	15.92
GM_2-20	2.92	569	12.1	25.27	3.64	270.6	12.0	31.65
GM_2-25	1.76	454	12.1	37.9	3.01	247.6	11.7	38.47
GM_2-20LS	2.33	536	12.1	32.21	3.92	258.1	11.8	34.25
				Corr. Coef	0.766	0.538	0.985	0.867

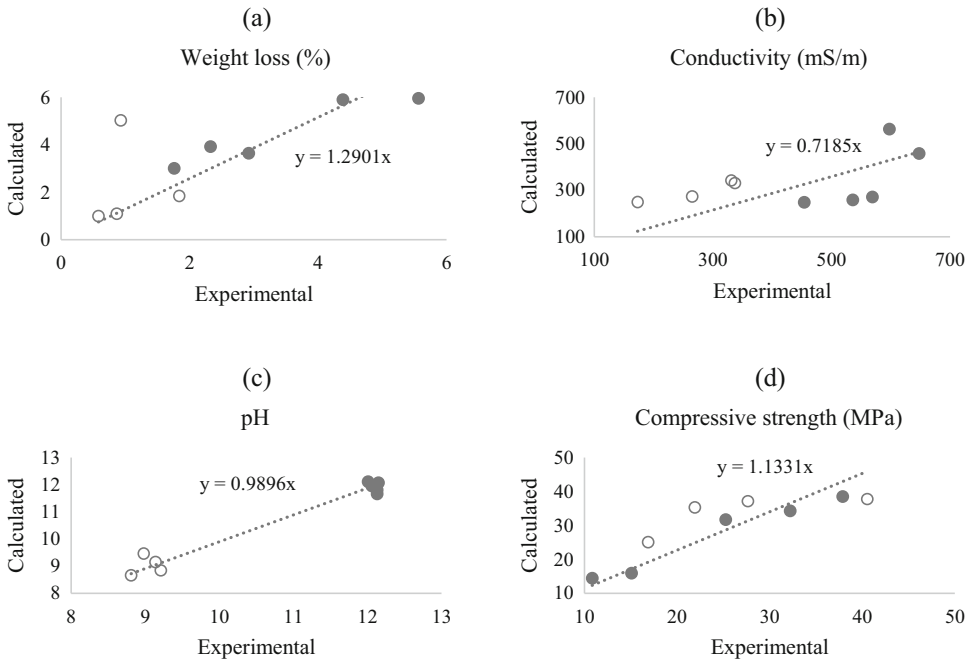

Figure 3 G-ANNs plots using VM-training: **a** weight loss; **b** conductivity; **c** pH; **d** average compressive strengths. The dashed line indicates the trendline passing for the origin. Legends: filled circle GM_2 series open circle GM_3 series.

G-ANNs

Analogously to the V-ANNs, the input data of GM series were used to train the G-ANNs. The obtained data, following the mathematical iterations of neural networks, evidence great capacity to predict the experimental results, as confirmed by the high correlation coefficients (i.e. about one) (Table 5). The correlations between the experimental (x axis) and calculated (y axis) data were plotted in Fig. 4, whose determination coefficients (R^2) of each trendlines demonstrated the good fitting. Moreover, the previsions on calculated data of VM samples, driven by GM training data, evidence an excellent predicting capacity (Fig. 5) with a correlation coefficient ranging around 0.71–0.98, whose highest value is linked to the pH (Fig. 5c) following by the compressive strengths (Fig. 5d).

Also, in this case, when considering the chemical aspects of the stabilization of the solid structure derived from the alkali activation process, the V-ANNs plots using GM-training indicate the sensitivity of the ghiara-based formulation upon the activating alkaline solution used. In plots reported in Fig. 5a, b, the ANNs are not predicting the linearity typical of the volcanic ash-based materials for the VM_2 series that were clearly overestimated by the prediction. These results suggest the strategy for optimizing the mix design using S_3 Na-silicate.

MLR results

V-MLR

With the aim to compare the ANN results with those of other more conventional statistical methods, multiple linear regression approach was carried out on the same sample sets. To evaluate the goodness of fitting, the calculated and experimental results of each physical property were plotted. These graphs are shown in Fig. 6. The line was forced to pass through the origin of Cartesian graph to avoid the negative intercepts obtained by least square iterations. If a good agreement is obtained, the points describe a straight line with slope and a R^2 close to one. The original (R^2) and R^2 adjusted coefficient, as well as the significance of variance analysis, are showed in Table 6 (see Table S1 for details on experimental and calculated results).

The first one is loosely interpreted as the proportion of the variability in the data explained by the model, the latter is a variation of the previous one that reflect the percentage of variation explained by only the independent variables that actually affect the dependent variable. The two parameters must be close [48]. The MLR of the weight loss showed a better fitting for the VM_2 series (Fig. 6a), although R^2 and R^2 adjusted are the lowest among all V-MLR, as well as confirmed by the highest significance

Table 5 Correlation between experimental and calculated data using G-training

Sample	Experimental data				Calculated data			
	weight loss (%)	Conductivity (mS/m)	pH	Comp. Strength (MPa)	weight loss (%)	Conductivity (mS/m)	pH	Comp. Strength (MPa)
GM_3-10	1.84	331	9.0	16.87	1.83	339.1	9.1	17.40
GM_3-15	0.93	337	9.1	21.93	0.98	327.0	9.0	20.77
GM_3-20	0.87	265	9.2	27.65	0.75	261.4	9.0	28.82
GM_3-25	0.58	173	8.8	40.54	0.68	195.1	9.0	38.62
GM_2-10	5.56	598	12.0	10.84	5.33	626.7	12.1	12.11
GM_2-15	4.38	648	12.2	15.09	4.49	620.5	12.1	14.34
GM_2-20	2.92	569	12.1	25.27	2.89	577.6	12.1	25.27
GM_2-25	1.76	454	12.1	37.9	1.75	451.2	12.1	38.47
GM_2-20LS	2.33	536	12.1	32.21	2.32	536.3	12.1	32.23
				Corr. Coef	0.998	0.995	0.997	0.995
VM_3-10	1.76	312	9.3	24.77	1.83	339.1	9.1	17.40
VM_3-15	5.18	372	9.5	37.79	0.98	327.0	9.0	20.77
VM_3-20	0.87	245	8.6	32.58	0.75	261.4	9.0	28.82
VM_3-25	0.91	261	8.5	39.59	0.68	195.1	9.0	38.62
VM_2-10	5.95	574.1	12.2	14.27	5.39	640.6	12.1	11.13
VM_2-15	4.68	574	12.2	15.32	4.83	633.9	12.1	11.55
VM_2-20	4.15	504	12.0	23.3	3.64	596.3	12.1	14.70
VM_2-25	3.23	261.1	12.0	38.03	2.49	526.9	12.1	29.48
VM_2-20LS	3.94	261.2	11.8	34.21	2.32	536.3	12.1	32.23
				Corr. Coef	0.715	0.713	0.982	0.873

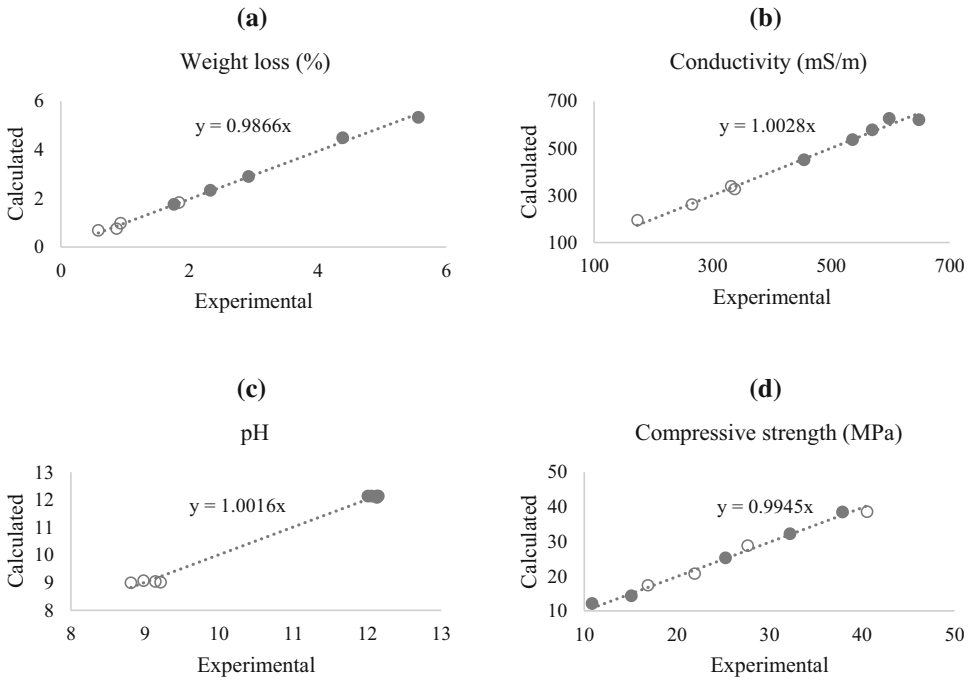

Figure 4 G-ANNs plots for each ANN created: **a** weight loss; **b** conductivity; **c** pH; **d** average compressive strengths. The dashed line indicates the trendline passing for the origin. Legends: filled circle GM_2 series open circle GM_3 series.

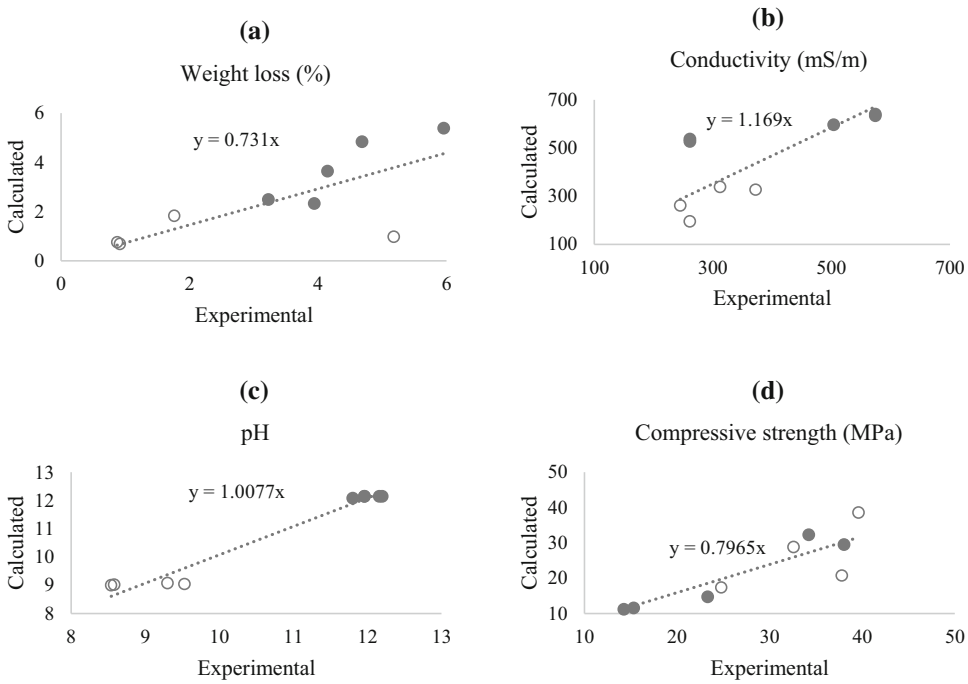

Figure 5 V-ANNs plots using GM-training: **a** weight loss; **b** conductivity; **c** pH; **d** average compressive strengths. The dashed line indicates the trendline passing for the origin. Legends: filled circle VM_2 series open circle VM_3 series.

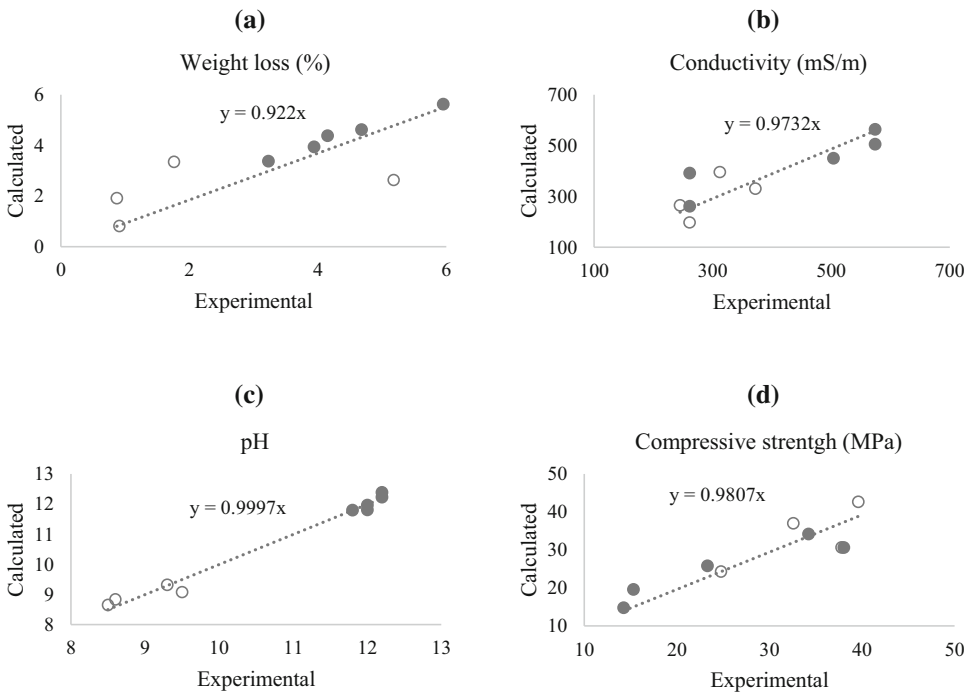

Figure 6 V-MLR plots for each MLR created: **a** weight loss; **b** conductivity; **c** pH; **d** average compressive strengths. The dashed line indicates the trendline passing for the origin. Legends: filled circle VM_2 series open circle VM_3 series.

(*F*) value (31%) (Table 6). The MLR of conductivity (Fig. 6b) and compressive strengths (Fig. 6d) showed a comparable behaviour, from which no series prevails and whose values suggest a poor correlation. Contrary, the MLR of pH evidences an excellent correlation (Fig. 6c), as highlighted by the significance (*F*) and the high determination coefficient close to one (Table 6). From the figures, it appears evident the higher correlation for VM_2 with respect to VM_3, probably because the activation with S_3 solution is not considered as reported in MLR design paragraph. Further, the lower correlation is for chemical properties (weight loss and conductivity) strictly related to reticulation degree in terms of amount of release

Table 6 MLR correlations of VM and GM samples for each physical property

	Weight loss (%)		Conductivity (mS/m)		pH		Compressive strength (MPa)	
	VM	GM	VM	GM	VM	GM	VM	GM
R^2	0.625	0.907	0.756	0.988	0.985	0.998	0.791	0.962
R^2 adjusted	0.250	0.814	0.513	0.975	0.970	0.996	0.582	0.925
Significance (F)	0.31616	0.02425	0.14905	0.00046	0.00068	0.00001	0.11257	0.00415

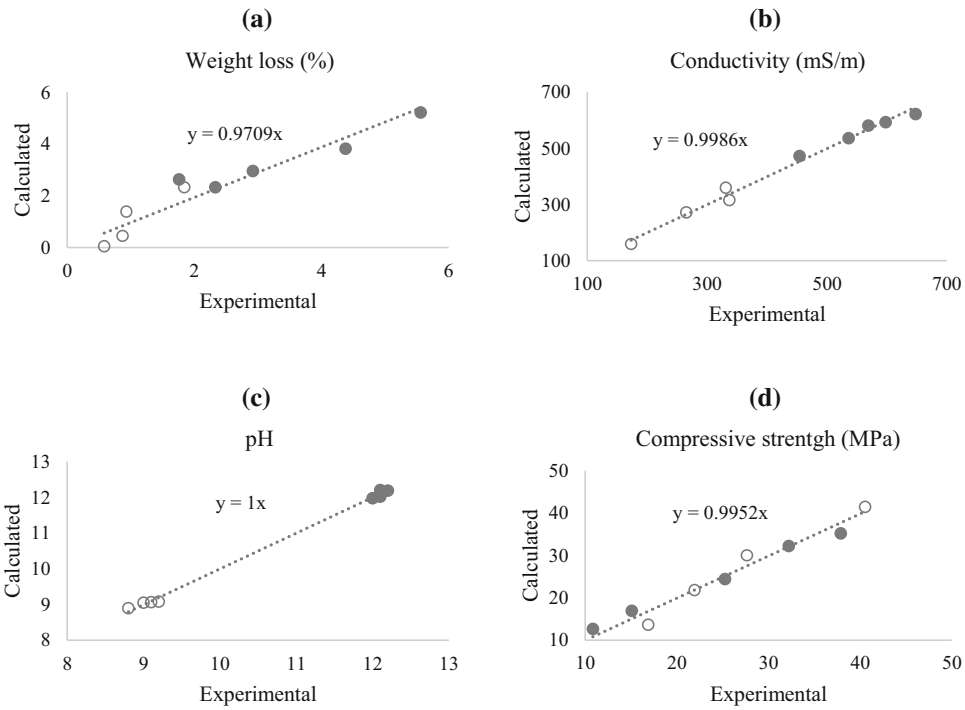

Figure 7 G-MLR plots for each MLR created: **a** weight loss; **b** conductivity; **c** pH; **d** average compressive strengths. The dashed line indicates the trendline passing for the origin. Legends: filled circle GM_2 series open circle GM_3 series.

ions. The pH values within the same series are less influenced due to the alkaline environment for all the compositions.

G-MLR

All G-MLR evidenced excellent correlations for each physical property, whose graphs are plotted in Fig. 7 while the coefficients in Table 6 (see Table S1 for details on experimental and calculated results). Regardless the values higher than 90%, some thin distinctions can be done. The MLR of weight loss showed the lowest agreement between calculated and experimental data (Fig. 7a), while those one of conductivity (Fig. 7b) and compressive strengths (Fig. 7d) are comparable and that one of pH the highest R^2 and agreement between calculated and experimental data (Fig. 7c; Table 6). Both GM_2 and GM_3 series highlighted the same behaviour and a great fitting, from which cannot be suppose none better network.

Conclusion

This work evidenced the possibility to use mathematical approaches, such as ANNs and MLR, to predict chemical stability of AAMs based on pyroclastic materials, whose main conclusions drawn are the following:

- For ANNs results, an excellent correlation among experimental and calculated data for the corresponding training series was found. Contrary, medium prediction capability for cross-correlations with the opposite volcanic series was

evidenced even if a further round of experimental data is needed to give quantitative values. Being ANN a more sophisticated method with respect to MLR, it is possible to verify the influence of the different activating solutions, resulting, thus, more powerful method than MLR as also reported for other application fields [49, 50].

- Concerning the chemical stability results, from the ANNs, the results appear evident that the alkaline solution with SiO_2/Na_2O molar ratio of 3 had a much stronger reticulation effect on GM samples with respect to volcanic ash that appeared almost insensitive to such molar ratio. For these VM samples, the reactivity is mainly due to the metakaolin fraction and proceed with the linearity expected from the % amount of MK in the mixture whatever the alkaline solution is used. In this context, the comparison of such ANNs results provides an interesting support to the interpretation of the role of the two different alkaline solutions used as activators.
- No suppositions on better network or on the best alkaline activation solution can be done according to MLR results due to the insensitivity of S_3, which was excluded by MLR iteration for the null and void influence. However, G-MLR evidenced an excellent correlation contrary to V-MLR.

Therefore, according to our dataset, ANN approach was more useful to suppose the variables which influence the chemical stability of these samples, contrary to the limitations occurred in MLR method. However, only thanks to the combination of both methods was possible to reach these conclusions. Finally, the compressive strength values of similar precursors and few known in the literature (in comparison with metakaolin and fly ash), such as volcanic deposits, are almost insensitive to the chemical network variations, differently from the results of weight loss, conductivity and pH that are strongly influenced by the degree of reticulation of the aluminosilicate matrix and in turn by Si/Al ratio of precursor mixtures. This study, as few others, on the chemical stability of AAMs provides a great contribution in the direction of durability and in-life mechanical performance of these class of materials. Any further optimization of AAMs mix design will start from those formulations that already have adopted the S_3 alkaline solution of Na-silicate.

Acknowledgements

This research is supported by the Advanced Green Materials for Cultural Heritage (AGM for CuHe) project (PNR fund with code: ARS01_00697; CUP E66C18000380005).

Funding

Open access funding provided by Università degli Studi di Catania within the CRUI-CARE Agreement.

Electronic supplementary material: The online version of this article (https://doi.org/10.1007/s10853-020-05250-w) contains supplementary material, which is available to authorized users.

References

[1] Davidovits J (1982) U.S. Patent No. 4,349,386

[2] Habert G, D'Espinose De Lacaillerie JB, Roussel N (2011) An environmental evaluation of geopolymer based concrete production: Reviewing current research trends. J Clean Prod 19:1229–1238. https://doi.org/10.1016/j.jclepro.2011.03.012

[3] Komnitsas KA (2011) Potential of geopolymer technology towards green buildings and sustainable cities. Proc Eng 21:1023–1032. https://doi.org/10.1016/j.proeng.2011.11.2108

[4] Liu Y, Shi C, Zhang Z, Li N (2019) An overview on the reuse of waste glasses in alkali-activated materials. Resour

Conserv Recycl 144:297–309. https://doi.org/10.1016/j.resconrec.2019.02.007

[5] Obonyo EA, Kamseu E, Lemougna PN et al (2014) A sustainable approach for the geopolymerization of natural iron-rich aluminosilicate materials. Sustain 6:5535–5553. https://doi.org/10.3390/su6095535

[6] Irfan Khan M, Azizli K, Sufian S, et al (2014) Geopolymers as a sustainable binder of 21st century: a review. d010. https://doi.org/10.3390/wsf-4-d010

[7] Lancellotti I, Ponzoni C, Barbieri L, Leonelli C (2013) Alkali activation processes for incinerator residues management. Waste Manag 33:1740–1749. https://doi.org/10.1016/j.wasman.2013.04.013

[8] Komnitsas K, Zaharaki D (2007) Geopolymerisation: A review and prospects for the minerals industry. Miner Eng 20:1261–1277. https://doi.org/10.1016/j.mineng.2007.07.011

[9] Contrafatto L (2017) Recycled Etna volcanic ash for cement, mortar and concrete manufacturing. Constr Build Mater 151:704–713. https://doi.org/10.1016/j.conbuildmat.2017.06.125

[10] Barone G, Mazzoleni P, Corsaro RA et al (2016) Nanoscale surface modification of Mt. Etna volcanic ashes. Geochim Cosmochim Acta 174:70–84. https://doi.org/10.1016/j.gca.2015.11.011

[11] Tchakoute HK, Elimbi A, Yanne E, Djangang CN (2013) Utilization of volcanic ashes for the production of geopolymers cured at ambient temperature. Cem Concr Compos 38:75–81. https://doi.org/10.1016/j.cemconcomp.2013.03.010

[12] Djobo JNY, Elimbi A, Tchakouté HK, Kumar S (2017) Volcanic ash-based geopolymer cements/concretes: the current state of the art and perspectives. Environ Sci Pollut Res 24:4433–4446. https://doi.org/10.1007/s11356-016-8230-8

[13] Lemougna PN, Wang K, tuo, Tang Q, et al (2018) Review on the use of volcanic ashes for engineering applications. Resour Conserv Recycl 137:177–190. https://doi.org/10.1016/j.resconrec.2018.05.031

[14] Kamseu E, Leonelli C, Perera DS et al (2009) Investigation of volcanic ash based geopolymers as potential building materials. Int Ceram Rev 58:136–140

[15] Battiato G (1988) Le malte del centro storico di Catania. Doc dell'Istituto Dipartimentale di Archit e Urban dell'Universita di Catania 16:85–107

[16] Sciuto Patti C (1896) Sui materiali da costruzioni più usati in Catania. Tipografia Editrice dell'Etna, Catania

[17] Belfiore CM, La Russa MF, Mazzoleni P et al (2010) Technological study of "ghiara" mortars from the historical city centre of Catania (Eastern Sicily, Italy) and petrochemical characterisation of raw materials. Environ Earth Sci 61:995–1003. https://doi.org/10.1007/s12665-009-0418-5

[18] Bultrini G, Fragala I, Ingo GM, Lanza G (2006) Mineropetrographic, thermal and microchemical investigation of historical mortars used in Catania (Sicily) during the XVII century A.D. Appl Phys A Mater Sci Process 83:529–536. https://doi.org/10.1007/s00339-006-3551-y

[19] de Ferri L, Santagati C, Catinoto M et al (2019) A multi-technique characterization study of building materials from the Exedra of S. Nicolò l'Arena in Catania (Italy). J Build Eng 23:377–387. https://doi.org/10.1016/j.jobe.2019.01.028

[20] Mazzoleni P (2007) The use of volcanic stone in architecture: example of Etnean region. Acta Vulcanol 18:141–144

[21] Barone G, Finocchiaro C, Lancellotti I et al (2020) Potentiality of the Use of Pyroclastic Volcanic Residues in the Production of Alkali Activated Material. Waste Biomass Valoriz. https://doi.org/10.1007/s12649-020-01004-6

[22] Xu H, Van Deventer JSJ (2000) The geopolymerisation of alumino-silicate minerals. Int J Miner Process 59:247–266. https://doi.org/10.1016/S0301-7516(99)00074-5

[23] Duxson P, Fernández-Jiménez A, Provis JL et al (2007) Geopolymer technology: the current state of the art. J Mater Sci 42:2917–2933. https://doi.org/10.1007/s10853-006-0637-z

[24] Lin YC, Fang X, Wang YP (2008) Prediction of metadynamic softening in a multi-pass hot deformed low alloy steel using artificial neural network. J Mater Sci 43:5508–5515. https://doi.org/10.1007/s10853-008-2832-6

[25] Ning L (2009) Artificial neural network prediction of glass transition temperature of fluorine-containing polybenzoxazoles. J Mater Sci 44:3156–3164. https://doi.org/10.1007/s10853-009-3420-0

[26] Garcia-Mateo C, Capdevila C, Caballero FG, De Andrés CG (2007) Artificial neural network modeling for the prediction of critical transformation temperatures in steels. J Mater Sci 42:5391–5397. https://doi.org/10.1007/s10853-006-0881-2

[27] Liujie X, Jiandong X, Shizhong W et al (2007) Artificial neural network prediction of heat-treatment hardness and abrasive wear resistance of High-Vanadium High-Speed Steel (HVHSS). J Mater Sci 42:2565–2573. https://doi.org/10.1007/s10853-006-1278-y

[28] Karakoç A, Keleş Ö (2020) A predictive failure framework for brittle porous materials via machine learning and geometric matching methods. J Mater Sci 55:4734–4747. https://doi.org/10.1007/s10853-019-04339-1

[29] Bondar D (2014) Use of a neural network to predict strength and optimum compositions of natural alumina-silica-based geopolymers. J Mater Civ Eng 26:499–503. https://doi.org/10.1061/(ASCE)MT.1943-5533.0000829

[30] Ling Y, Wang K, Wang X, Li W (2019) Prediction of engineering properties of fly ash-based geopolymer using artificial neural networks. Neural Comput Appl. https://doi.org/10.1007/s00521-019-04662-3

[31] Nazari A (2013) Artificial neural networks application to predict the compressive damage of lightweight geopolymer. Neural Comput Appl 23:507–518. https://doi.org/10.1007/s00521-012-0945-y

[32] Sadat MR, Muralidharan K, Zhang L (2018) Reactive molecular dynamics simulation of the mechanical behavior of sodium aluminosilicate geopolymer and calcium silicate hydrate composites. Comput Mater Sci 150:500–509. https://doi.org/10.1016/j.commatsci.2018.04.041

[33] Sadat MR, Bringuier S, Muralidharan K et al (2018) Atomic-scale dynamics and mechanical response of geopolymer binder under nanoindentation. Comput Mater Sci 142:227–236. https://doi.org/10.1016/j.commatsci.2017.10.026

[34] Lau CK, Lee H, Vimonsatit V et al (2019) Abrasion resistance behaviour of fly ash based geopolymer using nanoindentation and artificial neural network. Constr Build Mater 212:635–644. https://doi.org/10.1016/j.conbuildmat.2019.04.021

[35] Medri V, Fabbri S, Dedecek J et al (2010) Role of the morphology and the dehydroxylation of metakaolins on geopolymerization. Appl Clay Sci 50:538–545. https://doi.org/10.1016/j.clay.2010.10.010

[36] Haykin S (1994) Neural networks: a comprehensive foundation. Prentice Hall, Upper Saddle River

[37] Daniel G (2013) Principles of artificial neural networks - advanced series in circuits and systems (Vol. 7). World Scientific Publishing

[38] Pala M, Özbay E, Öztaş A, Yuce MI (2007) Appraisal of long-term effects of fly ash and silica fume on compressive strength of concrete by neural networks. Constr Build Mater 21:384–394. https://doi.org/10.1016/j.conbuildmat.2005.08.009

[39] Basheer IA, Hajmeer M (2000) Artificial neural networks: Fundamentals, computing, design, and application. J Microbiol Methods 43:3–31. https://doi.org/10.1016/S0167-7012(00)00201-3

[40] Shi H, Gao Y, Wang X (2010) Optimization of injection molding process parameters using integrated artificial neural network model and expected improvement function method. Int J Adv Manuf Technol 48:955–962. https://doi.org/10.1007/s00170-009-2346-7

[41] Liu SW, Huang JH, Sung JC, Lee CC (2002) Detection of cracks using neural networks and computational mechanics. Comput Methods Appl Mech Eng 191:2831–2845. https://doi.org/10.1016/S0045-7825(02)00221-9

[42] Günaydin HM, Doğan SZ (2004) A neural network approach for early cost estimation of structural systems of buildings. Int J Proj Manag 22:595–602. https://doi.org/10.1016/j.ijproman.2004.04.002

[43] Özcan F, Atiş CD, Karahan O et al (2009) Comparison of artificial neural network and fuzzy logic models for prediction of long-term compressive strength of silica fume concrete. Adv Eng Softw 40:856–863. https://doi.org/10.1016/j.advengsoft.2009.01.005

[44] Yaprak H, Karaci A, Demir I (2013) Prediction of the effect of varying cure conditions and w/c ratio on the compressive strength of concrete using artificial neural networks. Neural Comput Appl 22:133–141. https://doi.org/10.1007/s00521-011-0671-x

[45] Dou J, Yamagishi H, Pourghasemi HR et al (2015) An integrated artificial neural network model for the landslide susceptibility assessment of Osado Island, Japan. Nat Hazards 78:1749–1776. https://doi.org/10.1007/s11069-015-1799-2

[46] Saha A (2011) Data Mining in Excel. https://www.sites.google.com/site/sayhello2angshu/dminexcel

[47] Argyrous G (2011) Statistics for research: with a guide to SPSS. Sage Publications, London

[48] Montgomery DC (2013) Design and analysis of experiments. Wiley, London

[49] Perai AH, Moghaddam HN, Asadpour S et al (2010) A comparison of artificial neural networks with other statistical approaches for the prediction of true metabolizable energy of meat and bone meal. Poult Sci 89:1562–1568. https://doi.org/10.3382/ps.2010-00639

[50] Şahin M, Kaya Y, Uyar M (2013) Comparison of ANN and MLR models for estimating solar radiation in Turkey using NOAA/AVHRR data. Adv Sp Res 51:891–904. https://doi.org/10.1016/j.asr.2012.10.010